Neurochem Res (2012) 37:1315–1324
DOI 10.1007/s11064-012-0735-z

ORIGINAL PAPER

Structural Characterization of Monosialo-, Disialo- and Trisialo-gangliosides by Negative Ion AP-MALDI-QIT-TOF Mass Spectrometry with MS^n Switching

Emi Ito · Akio Tominaga · Hiroaki Waki · Kozo Miseki · Azusa Tomioka · Kazuki Nakajima · Kazuaki Kakehi · Minoru Suzuki · Naoyuki Taniguchi · Akemi Suzuki

Received: 2 November 2011 / Revised: 19 December 2011 / Accepted: 15 February 2012 / Published online: 6 March 2012

Abstract The atmospheric pressure matrix-assisted laser desorption/ionization (AP-MALDI) is a quite convenient soft ionization for biomolecules, keeping analytes atmospheric conditions instead of high vacuum conditions. In this study, an AP-MALDI ion source has been coupled to a quadrupole ion trap time-of-flight (QIT-TOF) mass spectrometer, which is able to perform MS^n analysis. We applied this system to the structural characterization of monosialogangliosides, GM1 (NeuAc) and GM2 (NeuAc), disialogangliosides, GD2 (NeuAc, NeuAc), GD1a (NeuAc, NeuAc) and GD1b (NeuAc, NeuAc) and trisialoganglioside GT1a (NeuAc, NeuAc, NeuAc). In this system, the negative ion mass spectra of MS, MS^2 and MS^3, a set of three mass spectra, were able to measure within 2 s per cycle. Thus, obtained results demonstrate that the negative ion mode MS, MS^2 and MS^3 spectra provided sufficient information for the determination of molecular weights, oligosaccharide sequences and ceramide structures, and indicate that the AP-MALDI-QIT-TOF mass spectrometry keeping analytes atmospheric conditions with MS^n switching is quite useful and convenient for structural analyses of various types of sialic acid-containing GSLs, gangliosides.

Keywords AP-MALDI · Negative ion · Mass spectrometry · Gangliosides · MS^n switching

Abbreviations

AP	Atmospheric pressure
MALDI	Matrix-assisted laser desorption/ ionization
QIT-TOF MS	Quadrupole ion trap time-of-flight mass spectrometry
GSLs	Glycosphingolipids

Introduction

Glycosphingolipids (GSLs) are a family of components of mammalian cell membranes along with membrane glycoproteins. Each GSL consists of a hydrophilic carbohydrate chain and a hydrophobic ceramide, and GSLs are related in

Special Issue: In honor of Bob Leedeen.

E. Ito · N. Taniguchi
Disease Glycomics Team, Systems Glycobiology Research Group, RIKEN, 2-1 Hirosawa, Wako-shi, Saitama 351-0198, Japan

A. Tominaga · H. Waki · K. Miseki · M. Suzuki
Shimadzu Corporation, 1 Nishinokyo-Kuwabaracho, Nakagyo-ku, Kyoto 604-8511, Japan

A. Tomioka
Research Center for Medical Glycoscience, National Institute of Advanced Industrial Science and Technology (AIST), 2-12 Tsukuba Central, 1-1-1 Umezono, Tsukuba, Ibaraki 305-8568, Japan

K. Nakajima · N. Taniguchi
Glycan Recognition Team, Systems Glycobiology Research Group, RIKEN, 2-1 Hirosawa, Wako-shi, Saitama 351-0198, Japan

K. Kakehi
School of Pharmacy, Kinki University, 3-4-1 Kowakae, Higashi-Osaka 577-8502, Japan

A. Suzuki (✉)
Institute of Glycoscience, Tokai University, 4-1-1 Kitakaname, Hiratsuka, Kanagawa 259-1292, Japan
e-mail: akmszk@tokai-u.jp

many cellular functions such as cell–cell recognition, cell growth and signal transduction [1–3]. Gangliosides are sialic acid-containing GSLs and abundant in neural cells, especially, in the synaptic region and are considered to play important roles in brain functions [4–9]. However, the actual roles of endogenous gangliosides in brain functions are still unknown and further studies are required. Recent studies have demonstrated that the diversity based on hydrophobic ceramide structures as well as the different carbohydrate structures of GSLs is critically important for the regulation of cellular functions [10–14]. Therefore, the development of methods for high throughput and reliable structural analyses of sugar chains and ceramides is required for the elucidation of the physiological roles of GSLs or gangliosides.

Mass spectrometry is an indispensable tool for the structural characterization of GSLs, because it can provide information on molecular weights, carbohydrate sequences and ceramide structures. Matrix-assisted laser desorption/ionization (MALDI) is a widely used ionization method for the analysis of biomolecules. MALDI-QIT-TOF (quadrupole ion trap time-of-flight) mass spectrometry, which enables to perform MS^n analysis, has been developed for the fine structural characterization of organic compounds [15–17]. In addition, atmospheric pressure (AP) MALDI has several advantages over MALDI, easy sample handling and no need of analytes kept *in vacuo* [18–22]. Therefore, AP-MALDI does not require consideration for alteration of biological samples in vacuum state.

In this study, a commercially available AP-MALDI ion source has been coupled to a QIT-TOF mass spectrometer for the structural characterization of monosialo, disialo and trisialogangliosides. By this system, the negative ion mode mass spectra of MS, MS^2 and MS^3 are able to be provided within 2 s, and informative fragmentation patterns of six kinds of ganglioside including monosialo, disialo and trisialoganglioside have been obtained. We report here structural characterization of six gangliosides by AP-MALDI-QIT TOF mass spectrometry with MS^n switching.

Materials and Methods

Materials

GM1 (NeuAc) was prepared from bovine brain and GM2 (NeuAc) from the brain of a patient with Tay-Sachs disease [23]. GD2 (NeuAc, NeuAc), GD1a (NeuAc, NeuAc) and GD1b (NeuAc, NeuAc) from bovine brain, and GT1a (NeuAc, NeuAc, NeuAc) from human brain were purchased from Funakoshi Co., Ltd. (Tokyo, Japan). The matrix used for MALDI ionization, α-cyano-4-hydroxycinnamic acid (α-CHCA), was purchased from Wako Pure Chemicals Industries (Osaka, Japan). All solvents used for the MS analysis were of HPLC grade.

Sample Preparation for the Measurement of Mass Spectra of Gangliosides

GM1, GM2, GD2, GD1a, GD1b and GT1a were dissolved as 1 mg/ml in methanol, and diluted tenfold with distilled water. A 30 mM solution of α-CHCA was prepared with acetonitrile and methanol (1:1, v/v). Equal volume of each ganglioside solution and 30 mM α-CHCA solution was mixed to prepare 50 ng/μl of ganglioside solutions. After mixing, 1 μl of ganglioside-matrix solution was applied on a gold-coated MALDI target plate, and dried up at room temperature.

Atmospheric Pressure Matrix-Assisted Laser Desorption/Ionization Quadrupole Ion Trap Time-of-Flight (AP-MALDI-QIT-TOF) Mass Spectrometry

All experiments were performed on a LCMS-IT-TOF quadrupole ion trap time-of-flight mass spectrometer (Shimadzu, Kyoto, Japan) equipped with an AP-MALDI source (Mass Technologies, Burtonsville, MD). This instrument consists of five main sections: an ion source, a lens system, an ion trap, a reflectron time-of-flight mass analyzer and a N_2 laser control unit. Ions from the ion source passed through the lens system, accumulated in an ion trap, and then were discharged to TOF. A pulsed gas, Ar, was used for ion cooling and collision-induced dissociation. To keep mass precision, the temperature inside of the instrument is controlled within 40 ± 0.3°C. N_2 laser at 337 nm (10 Hz) was focused on sample zones on a MALDI target plate, and the size of the laser spot was approximately 200 μm. High voltage supplied to the MALDI target plate was ±3.5 kV. The distance between the MALDI target plate and the heated capillary located on the entrance of ion introducing block, which was kept at 250°C, was 2 mm. The mass spectrum measurement cycle time for obtaining all negative ion MS, MS^2 and MS^3 spectra of each ganglioside, including ion accumulating time, ion cooling time, precursor ion selecting time, and collision induced dissociation time, was set to 1.9 s/cycle.

Results

Negative Ion AP-MALDI-QIT-TOF MS, MS^2 and MS^3 Spectra of Monosialogangliosides, GM1 (NeuAc) and GM2 (NeuAc)

Table 1 lists the structure of monosialo, disialo and trisialogangliosides used in this study. Figure 1 shows the AP-MALDI-QIT-TOF MS, MS^2 and MS^3 mass spectra of

Table 1 Structures of monosialogangliosides (GM1 and GM2), disialogangliosides (GD2, GD1a and GD1b) and trisialogangliosides (GT1a), containing N-acetyl neuraminic acid (NeuAc)

GM1	Galβ1-3GalNAcβ1-4(NeuAcα2-3)Galβ1-4Glcβ1-1′Cer
GM2	GalNAcβ1-4(NeuAcα2-3)Galβ1-4Glcβ1-1′Cer
GD2	GalNAcβ1-4(NeuAcα2-8NeuAcα2-3)Galβ1-4Glcβ1-1′Cer
GD1a	NeuAcα2-3Galβ1-3GalNAcβ1-4(NeuAcα2-3)Galβ1-4Glcβ1-1′Cer
GD1b	Galβ1-3GalNAcβ1-4(NeuAcα2-8NeuAcα2-3)Galβ1-4Glcβ1-1′Cer
GT1a	NeuAcα2-8NeuAcα2-3Galβ1-3GalNAcβ1-4(NeuAcα2-3)Galβ1-4Glcβ1-1′Cer

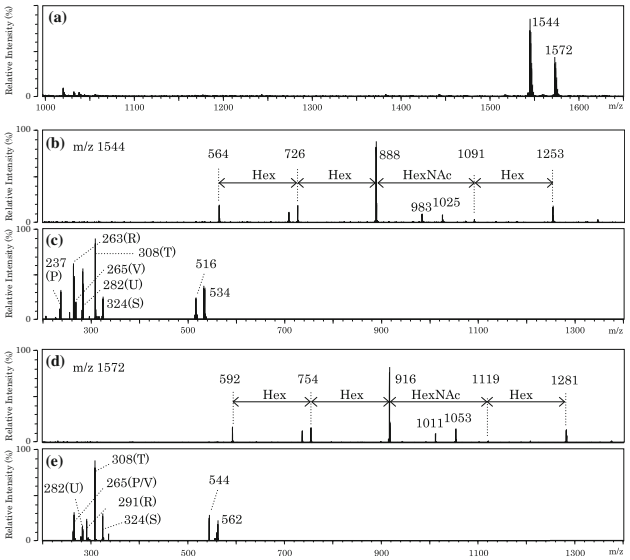

Fig. 1 MS, MS^2 and MS^3 spectra of GM1 by Negative ion MS^n switching AP-MALDI-QIT-TOF MS. **a** MS spectrum of GM1 (NeuAc); **b** MS^2 spectrum selecting as the first precursor ion at *m/z* 1,544; **c** MS^3 spectrum selecting as the second precursor ion at *m/z* 564; **d** MS^2 spectrum selecting another molecular species of GM1 as the first precursor ion at *m/z* 1,572; **e** MS^3 spectrum selecting as the second precursor ion at *m/z* 592. Annotations for *P*, *R*, *T*, *V*, *U* and *S* are shown in Fig. 2

GM1 containing N-acetylneuraminic acid (NeuAc) in the negative ion mode. In the MS spectrum of GM1, deprotonated molecular ions ($[M-H]^-$) of the major molecular species of GM1 were detected at *m/z* 1,544 and 1,572, as shown in Fig. 1a. MS^2 spectrum selecting the ion at *m/z* 1,544 as the precursor ion exhibits product ions at 1,253, 1,091, 888, 726 and 564, which are responsible for $[M-H-NeuAc]^-$, $[M-H-NeuAc-Hex]^-$, $[M-H-NeuAc-Hex-HexNAc]^-$, $[M-H-NeuAc-Hex-HexNAc-Hex]^-$ and $[M-H-NeuAc-Hex-HexNAc-Hex-Hex]^-$, respectively (Fig. 1b). In this mass spectrum, two ions observed at *m/z* 983 and 1,025, which are presumably responsible for the ring cleavage of II-GalNAc residue at the non-reducing end of asialo-GM1 backbone structure, might be assigned as $[^{2,3}X_2-2H_2O]^-$ and $[^{0,1}X_2-2H_2O]^-$, respectively. In the MS^3 spectrum selecting the ceramide ion at *m/z* 564, product ions were observed at *m/z* 324, 308, 282, 265, 263 and 237 (Fig. 1c) which are assigned to be S, T, U, V, R and P ions, respectively, according to the annotation by Ann and Adams and Lee et al. [24–26], shown in Fig. 2. These characteristic product ion analyses are able to identify as d18:1 sphingosine and as C18:0 fatty acid. Similarly, in the MS^2 spectrum selecting another deprotonated molecular ion of GM1 at *m/z* 1,572 as the precursor ion were observed the ions at *m/z* 1,281, 1,119, 916, 754, and 592, which are responsible for $[M-H-NeuAc]^-$, $[M-H-NeuAc-Hex]^-$, $[M-H-NeuAc-Hex-HexNAc]^-$, $[M-H-NeuAc-Hex-HexNAc-Hex]^-$ and [M−H−NeuAc−Hex−HexNAc−Hex−Hex], respectively (Fig. 1d). Ions at *m/z* 1,011 and 1,053 might be assigned as $[^{2,3}X_2-2H_2O]^-$ and $[^{0,1}X_2-2H_2O]^-$ of asialo-GM1 core structure, respectively. In the MS^3 spectrum selecting the ceramide ion at *m/z* 592, ions at *m/z* 324, 308, 282, 291 and 265, which are assigned to be S, T, U, R and P/V ions [24–26]. These characteristic product ion analysis enables to identify sphingosine base as d20:1 and fatty acid as C18:0. These results indicate that the MS^n analysis in the negative ion mode provides information on the molecular weights by MS, the oligosaccharide sequences

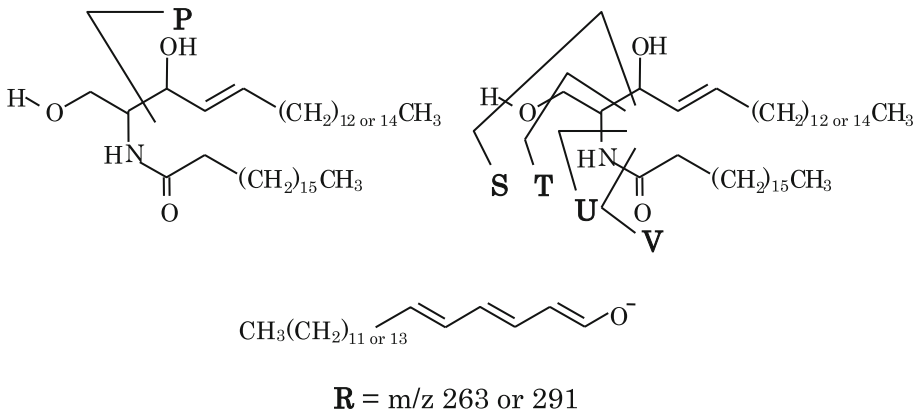

Fig. 2 Characteristic product ions generated from ceramide moiety based on the nomenclature by Ann and Adams [24, 25] and reported by Lee et al. [26]

deduced from the ions due to elimination of successive elimination of oligosaccharide moieties from the deprotonated ion by MS^2, and the ceramide structure from the ions derived from the fatty acid and sphingosine by MS^3. Finally, GM1 could be clearly confirmed to contain two major molecular species carrying d18:1–C18:0 and d20:1–C18:0.

Figure 3 shows MS, MS^2 and MS^3 spectra of GM2 (NeuAc) in the negative ion mode. The deprotonated molecular ions of GM2 ($[M-H]^-$) were observed at *m/z* 1,382 and 1,410. In the MS^2 spectrum of GM2 selecting as the precursor ion at *m/z* 1,382, the ions at *m/z* 1,091 ($[M-H-NeuAc]^-$), 888 ($[M-H-NeuAc-HexNAc]^-$), 726 ($[M-H-NeuAc-HexNAc-Hex]^-$) and 564 ($[M-H-NeuAc-HexNAc-Hex-Hex]^-$) were observed (Fig. 3b). MS^3 spectra selecting the ceramide ions at *m/z* 564, as shown in Fig. 4c, showed significant peaks at *m/z* 324 (S), 308 (T), 282 (U) 265 (V), 263 (R) and 237 (P), which are characterized ceramide consisting of d18:1 sphingosine and C18:0 fatty acid. Similarly, in the MS^2 mass spectrum of GM2 selecting the ion at *m/z* 1,410, the ions at *m/z* 1,191 ($[M-H-NeuAc]^-$), 916 ($[M-H-NeuAc-HexNAc]^-$), 754 ($[M-H-NeuAc-HexNAc-Hex]^-$) and 592 ($[M-H-NeuAc-HexNAc-Hex-Hex]^-$) were observed (Fig. 3d). The ions, which might be responsible for ring cleavage of II-GalNAc of asialo-GM1 backbone, were not observed in the MS^2 mass spectra of GM2 (Fig. 3b, d). MS^3 spectra selecting the ceramide ion at *m/z* 592, as shown in Fig. 4e, showed significant peaks at 324 (S), 308 (T), 291 (R), 282 (U) and 265 (P/V), which were assigned sphingosine as d20:1 and fatty acid as C18:0 by calculation of the fragment ions derived from ceramide.

Negative ion AP-MALDI-QIT-TOF MS, MS^2 and MS^3 Spectra of Disialogangliosides, GD2 (NeuAc, NeuAc), GD1a (NeuAc, NeuAc) and GD1b (NeuAc, NeuAc)

In the negative ion mass spectrum of GD2 shown in Fig. 4a, the deprotonated molecular ions ($[M-H]^-$), dehydrate ions from the deprotonated molecules ($[M-H-H_2O]^-$) and ions due to elimination of NeuAc from the deprotonated molecules ($[M-H-NeuAc]^-$) were observed at *m/z* 1,673 and 1,701, 1,655 and 1,683 and 1,382 and 1,410, respectively. In the MS^2 spectrum selecting the ion at *m/z* 1,382, the ions at *m/z* 1,091, 888, 726 and 564, which due to the eliminations of NeuAc, NeuAc and HexNAc, NeuAc and HexNAc-Hex and NeuAc and HexNAc-Hex-Hex from ($[M-H-NeuAc]^-$), were detected, respectively. In the MS^3 spectra selecting the ceramide ions at *m/z* 564, as shown in Fig. 4c, ions at *m/z* 308 (T), 282 (U) 265 (V), 263 (R) and 237 (P), which were assigned sphingosine as d20:1 and fatty acid as C18:0 by calculation of ions derived from ceramide fragmentation, were observed clearly. Similarly, as shown in Fig. 4d, in the MS^2 spectrum selecting another [M−H−NeuAc] ion at *m/z* 1,410, the ions at *m/z* 1,191, 916, 754 and 592, which due to the eliminations of NeuAc, NeuAc and HexNAc, NeuAc and HexNAc-Hex and NeuAc and HexNAc-Hex-Hex from

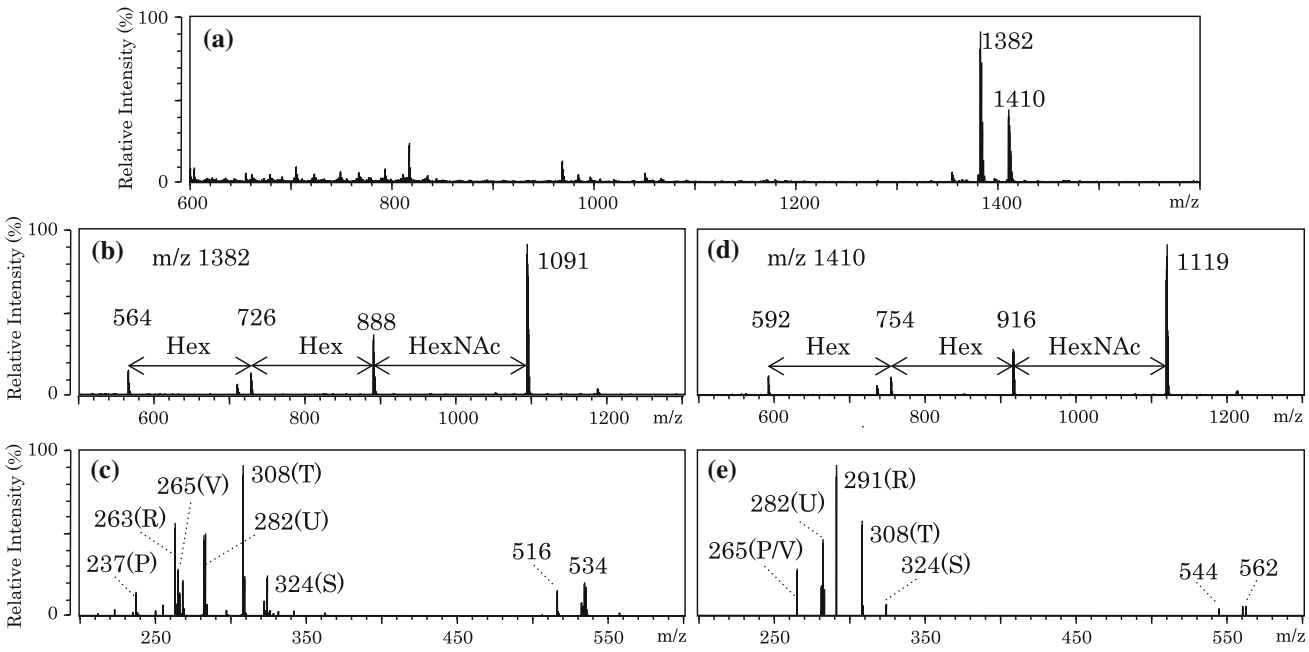

Fig. 3 MS, MS^2 and MS^3 spectra of GM2 by Negative ion MS^n switching AP-MALDI-QIT-TOF MS. **a** MS spectrum of GM2 (NeuAc); **b** MS^2 spectrum selecting as the first precursor ion at *m/z* 1,382; **c** MS^3 spectrum selecting as the second precursor ion at *m/z* 564; **d** MS^2 spectrum selecting another molecular species of GM2 as the first precursor ion at *m/z* 1,410; **e** MS^3 spectrum selecting as the second precursor ion at *m/z* 592. Annotations for *P*, *R*, *T*, *V*, *U* and *S* are shown in Fig. 2

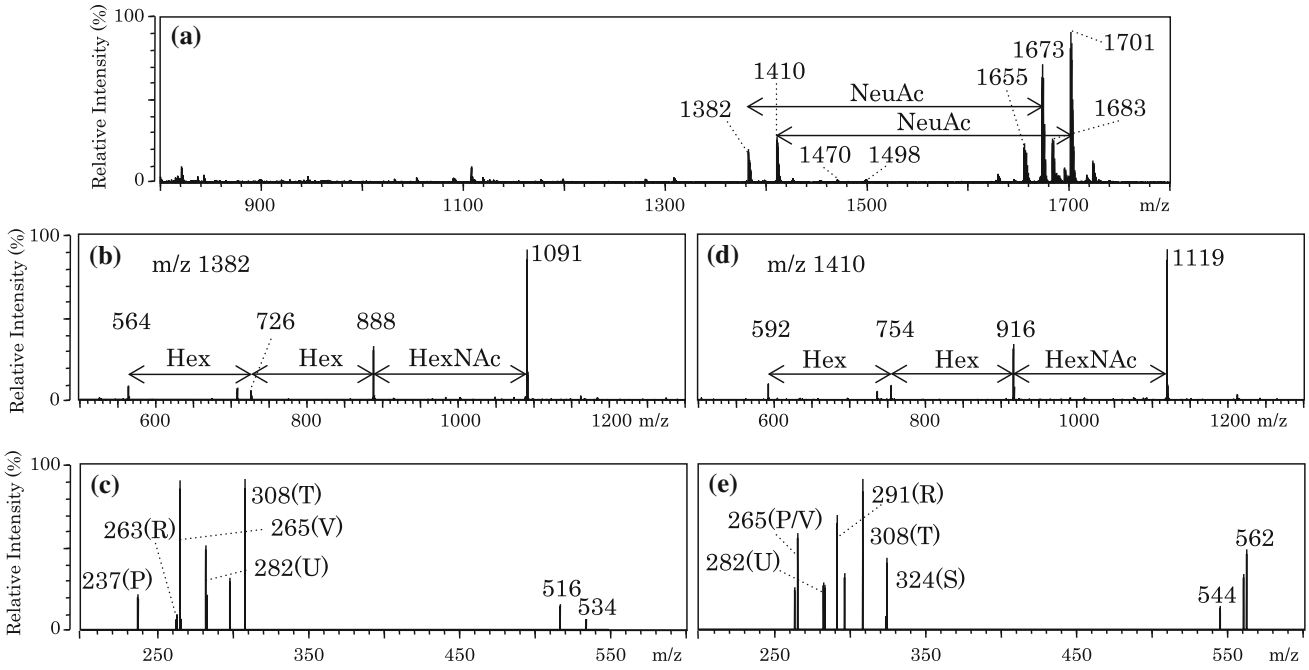

Fig. 4 MS, MS^2 and MS^3 spectra of GD2 by Negative ion MS^n switching AP-MALDI-QIT-TOF MS. **a** MS spectrum of GD2 (NeuAc, NeuAc); **b** MS^2 spectrum selecting as the first precursor ion at *m/z* 1,382; **c** MS^3 spectrum selecting as the second precursor ion at *m/z* 564; **d** MS^2 spectrum selecting another molecular species of GD2 as the first precursor ion at *m/z* 1,410; **e** MS^3 spectrum selecting as the second precursor ion at *m/z* 592. Annotations for *P*, *R*, *T*, *V*, *U* and *S* are shown in Fig. 2

([M−H−NeuAc]$^-$), respectively, were observed. In the MS^3 spectrum selecting the ceramide ions at *m/z* 592, as shown in Fig. 4e, significant peaks at 324 (S), 308 (T), 291 (R), 282 (U) and 265 (P/V) were assigned as d20:1 sphingosine and as C18:0 fatty acid by calculation of ceramide cleavage. Thus, it was also confirmed that two major molecular species of GD2 were d18:1–C18:0 and d20:1–C18:0.

Figure 5 shows MS, MS^2 and MS^3 spectra of GD1a and GD1b in the negative ion mode. In the MS spectrum of GD1a shown in Fig. 5a, deprotonated molecular ions ([M−H]$^-$) at *m/z* 1,835 and 1,863 were detected clearly, and ions due to elimination of one of two NeuAc from the molecular related ions ([M−H−NeuAc]$^-$) were also observed at *m/z* 1,544 and 1,572 with strong intensity. In addition, the fragment ions were observed at *m/z* 1,382 and 1,410, and at *m/z* 1,179 and 1,207, which are responsible for the elimination of Gal and Gal-GalNAc from [M−H−NeuAc]$^-$, respectively. In the MS spectrum of GD1b shown in Fig. 5f, deprotonated molecular ions were detected at *m/z* 1,835 and 1,863 with each dehydrated ion at *m/z* 1,817 and 1,845, and ions due to elimination of 1 mole of NeuAc from the deprotonated molecules were also observed at *m/z* 1,544 and 1,572. Furthermore, ions with week intensity due to the elimination of terminal Gal and Gal-GalNAc from the deprotonated molecules ([M−H]$^-$) were detected at *m/z* 1,673 and 1,701, and at *m/z* 1,470 and 1,498, respectively. The comparison of MS spectra of GD1a and GD1b indicates that the fragment ions at *m/z* 1,382 and 1,410, and at *m/z* 1,179 and 1,207 are characteristic of GD1a structure, and the ions at *m/z* 1,673 and 1,701, and at *m/z* 1,470 and 1,498 are characteristic of GD1b structure.

In the MS^2 spectra of GD1a and GD1b selecting each ion at *m/z* 1,544 and 1,572 ([M−H−NeuAc]$^-$), ions due to [M−H−2NeuAc]$^-$, [M−H−2NeuAc−Hex]$^-$, [M−H−2NeuAc−Hex−HexNAc]$^-$, [M−H−2NeuAc−Hex−HexNAc−Hex]$^-$ and [M−H−2NeuAc−Hex−HexNAc−Hex−Hex]$^-$ were observed clearly at *m/z* 1,253 and 1,281, 1,091 and 1,119, 888 and 916, 726 and 754 and 564 and 592 (Fig. 5b, d for GD1a, and Fig. 5g, i for GD1b), respectively. In each MS^2 mass spectrum, ions which might be responsible for $[^{2,3}X_2-2H_2O]^-$ and $[^{0,1}X_2-2H_2O]^-$ of asialo-GM1 core structure were observed clearly at *m/z* 983 and 1,025 (Fig. 5b for GD1a, 5g for GD1b), and *m/z* 1,011 and 1,053 (Fig. 5d for GD1a, 5i for GD1b), respectively.

In the MS^3 spectra of GD1a and GD1b selecting ceramide ion at *m/z* 564 (Fig. 5c for GD1a, 5h for GD1b), ions derived from ceramide cleavage were obtained at *m/z* 324 (S), 308 (T), 282 (U), 265 (V), 263 (R) and 237 (P), respectively, which were assigned as d18:1–C18:0 ceramides. In the MS^3 spectra of GD1a and GD1b selecting another ceramide ion at *m/z* 592 (Fig. 5e for GD1a, 5j for GD1b), ions responsible for the ceramide cleavage were observed at *m/z* 324 (S), 308 (T), 291 (R), 282 (U) and 265 (P/V), which were assigned as d20:1–C18:0 ceramides by calculation of ceramide cleaved ions.

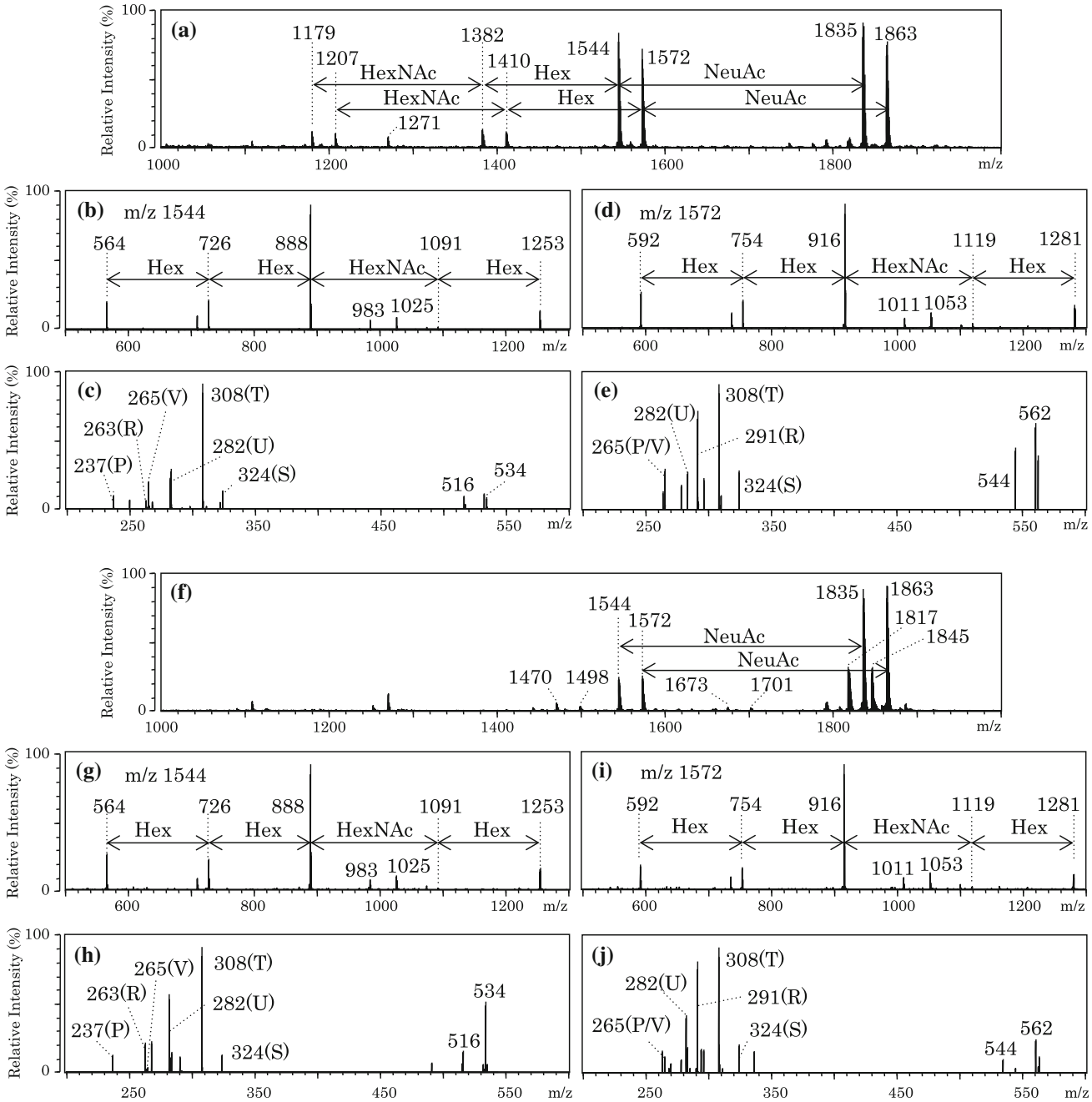

Fig. 5 MS, MS^2 and MS^3 spectra of GD1a and GD1b by Negative ion MS^n switching AP-MALDI-QIT-TOF MS. **a** MS spectrum of GD1a (NeuAc, NeuAc); **b** MS^2 spectrum selecting as the first precursor ion at *m/z* 1,544; C, MS^3 spectrum selecting as the second precursor ion at *m/z* 564; **d** MS^2 spectrum selecting another molecular species of GD1a as the first precursor ion at *m/z* 1,572; **e** MS^3 spectrum selecting as the second precursor ion at *m/z* 592; **f** MS spectrum of GD1b (NeuAc, NeuAc); **g** MS^2 spectrum selecting as the first precursor ion at *m/z* 1,544; **h** MS^3 spectrum selecting as the second precursor ion at *m/z* 564, **i** MS^2 spectrum selecting another molecular species of GD1b as the first precursor ion at *m/z* 1,572; **j** MS^3 spectrum selecting as the second precursor ion at *m/z* 592. Annotations for *P*, *R*, *T*, *V*, *U* and *S* are shown in Fig. 2

Negative Ion AP-MALDI-QIT-TOF MS, MS^2 and MS^3 Spectra of Trisialoganglioside, GT1a (NeuAc, NeuAc, NeuAc)

Figure 6 shows MS, MS^2 and MS^3 spectra of GT1a in the negative ion mode. In the MS spectrum of GT1a, the deprotonated molecular ions ($[M-H]^-$) are detected at *m/z* 2,126 and 2,154 with each dehydrated peak at *m/z* 2,108 and 2,136 (Fig. 6a), in addition, ions due to elimination of one of three NeuAc from the molecular related ions were observed at *m/z* 1,835 and 1,863. Furthermore, ions due to elimination of another NeuAc and

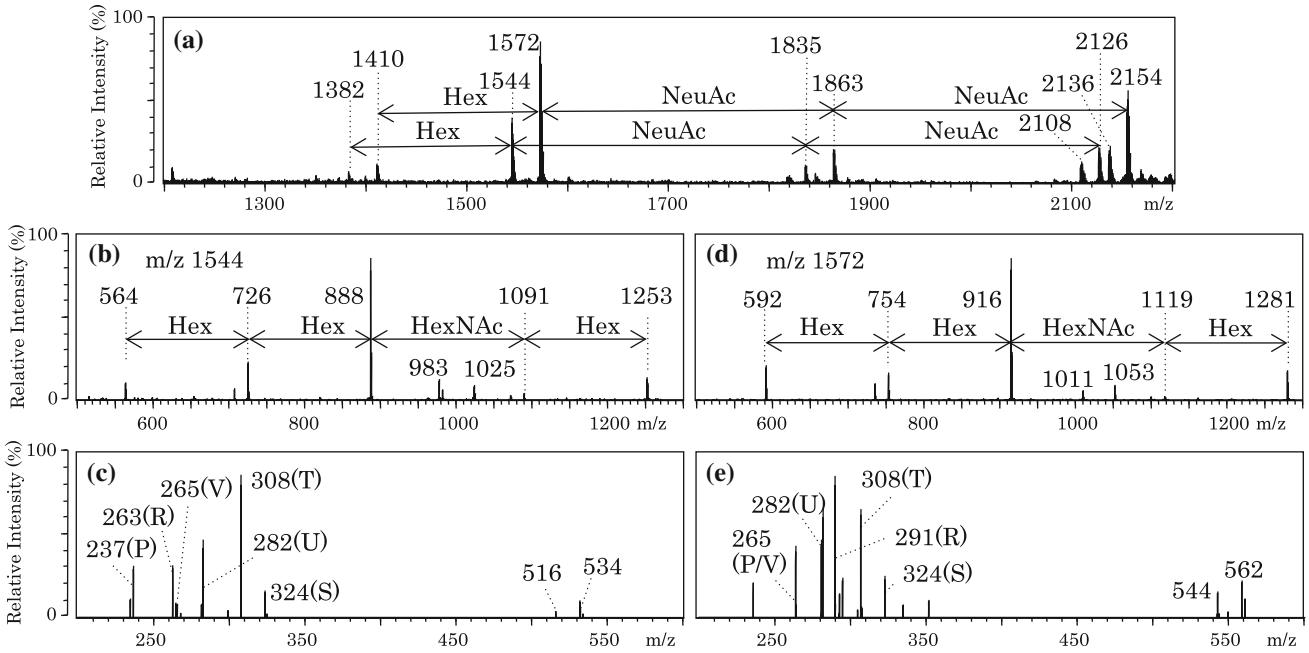

Fig. 6 MS, MS^2 and MS^3 spectra of GT1a by Negative ion MS^n switching AP-MALDI-QIT-TOF MS. **a** MS spectrum of GT1a (NeuAc, NeuAc, NeuAc); **b** MS^2 spectrum selecting as the first precursor ion at *m/z* 1,544; **c** MS^3 spectrum selecting as the second precursor ion at *m/z* 564; **d** MS^2 spectrum selecting another molecular species of GT1a as the first precursor ion at *m/z* 1,572; **e** MS^3 spectrum selecting as the second precursor ion at *m/z* 592. Annotations for *P*, *R*, *T*, *V*, *U* and *S* are shown in Fig. 2

$[M-H-2NeuAc-Hex]^-$ were obtained at *m/z* 1,544 and 1,572, and *m/z* 1,382 and 1,410, respectively. In the MS^2 spectra selecting the ions at *m/z* 1,544 and 1,572 ($[M-H-2NeuAc]^-$), ions were detected due to elimination of another NeuAc at *m/z* 1,253 and 1,281, NeuAc and Hex at *m/z* 1,091 and 1,119, NeuAc and Hex-HexNAc at *m/z* 888 and 916, NeuAc and Hex-HexNAc-Hex at *m/z* 726 and 754 and NeuAc and Hex-HexNAc-Hex-Hex at *m/z* 564 and 592, as shown in Fig. 6b, d. The ions detected at *m/z* 983 and 1,025 in Fig. 6b, and *m/z* 1,011 and 1,053 in Fig. 6d might be assigned as $[^{2,3}X_2-2H_2O]^-$ and $[^{0,1}X_2-2H_2O]^-$, respectively, and these ions might be produced by the cross-ring cleavage of GalNAc of asialo-GM1 back bone structures. In the MS^3 spectra selecting the ceramide ion at *m/z* 564 and 592, the same significant peaks were detected those of other gangliosides, as shown in Fig. 6c, e. Thus, by the analyses of the fragment ions derived from sphingosine base and fatty acid, the ceramide structures of GT1a consist of two molecular species, d18:1–18:0 and d20:1–18:0.

Discussion

Vacuum MALDI mass spectrometers are a widely used tool in glycomic approach [27, 28], and the system is quite useful for the structural characterization of gangliosides. AP-MALDI mass spectrometry holds an advantage over vacuum MALDI, that is, analytes are handled under atmospheric pressure conditions without the loading of the MALDI target plate *in vacuo*. The AP-MALDI ion source is a commercially available as an external ion source and any types of MS instruments are able to be coupled with minor modifications [29].

In this study, AP-MALDI-QIT-TOF mass spectrometry with MS^n switching has been applied to structural characterization of typical acidic GSLs; GM1, GM2, GD2, GD1a, GD1b and GT1a. This MS system can provide the positive and negative ion spectra with high speed polarity switching of MS, MS^2 and MS^3, a set of six kinds of spectra, within 4 s per cycle. If it is not known whether the positive or negative ion mass spectra can provide useful information for the structural characterization of analytes, we can operate this system using both ion modes quite easily. First, we measured mass spectra of GM1 by the AP-MALDI-QIT-TOF mass spectrometry with polarity and MS^n switching. As a result, in the positive ion mode MS spectrum, the sodium adduct molecular ions of GM1 containing d18:1–18:0 and d20:1–18:0 were detected at *m/z* 1,568 and 1,596, concurrently, ions due to elimination of NeuAc from the sodium adduct molecular ions were observed at *m/z* 1,277 and 1,305, as shown in Fig. 7a. In the MS^2 mass spectra selecting the ions at *m/z* 1,277 and 1,305, ions due to elimination of Hex and HexNAc were observed at *m/z* 1,115 and 912 (Fig. 7b) and *m/z* 1,143 and 940 (Fig. 7d), respectively. However, structural characterization of ceramide moieties of GM1 selecting

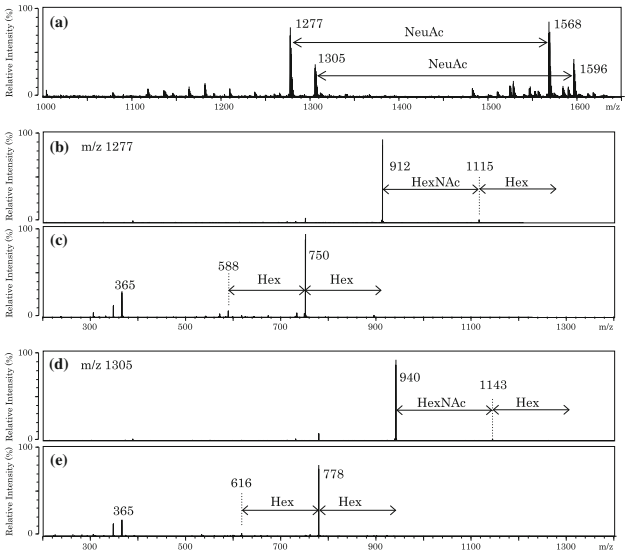

Fig. 7 MS, MS^2 and MS^3 spectra of GM1 (NeuAc) by Positive ion MS^n switching AP-MALDI-QIT-TOF MS. **a** MS spectrum of GM1 (NeuAc); **b** MS^2 spectrum selecting as the first precursor ion at *m/z* 1,277; **c** MS^3 spectrum selecting as the second precursor ion at *m/z* 912; **d** MS^2 spectrum selecting another molecular species of GM1 as the first precursor ion at *m/z* 1,305; **e** MS^3 spectrum selecting as the second precursor ion at *m/z* 940

m/z 912 and 940 as precursor ions were impossible because of poor fragment ions due to ceramide cleavage, as shown in Fig. 7c, e. That is the reason why we selected negative ion mode not positive ion mode for the measurements of mass spectra of monosialo, disialo and trisialogangliosides by the AP-MALDI-QIT-TOF mass spectrometry with MS^n switching at 1.9 s/cycle. Recently, Ikeda et al. reported the quantitative analysis of ganglioside molecular species by LC-ESI MS/MS with MRM (Multiple Reaction Monitoring) method [30, 31]. MRM is a useful method for quantitative analysis, but it is difficult to provide the detailed structural information on ceramide moieties, because the MS^3 spectra selecting the ceramide ions as the precursor could not be obtained by the triple-quadrupole linier ion trap mass spectrometer. Nakamura et al. [32] reported structural characterization of neutral glycosphingolipids by thin-layer chromatography (TLC) coupled to MALDI-QIT-TOF MS^2. By coupling TLC-immunostaining of GSLs to MALDI-QIT-TOF MS^2, they could identify both oligosaccharide sequences and sphingosine structures, however, they could not obtained detail information on the ceramide structures.

In the negative ion AP-MALDI-QIT-TOF mass spectra of monosilo, disialo and trisilogangliosides, alkaline metal adduct ions, e.g. sodium adduct ions ($[M+Na-2H]^-$ and $[M+2Na-3H]^-$) and/or potassium adduct ions ($[M+K-2H]^-$ and $[M+2K-3H]^-$) were not detectable or detectable with quite week intensity as shown in Figs. 1a, 3a, 4a, 5a, f, and 6a. These results suggest that determination of molecular weights of gangliosides is quite easy compared with that of vacuum MALDI-MS [33–36] which was widely used in glycobiology field. Furthermore, in the case of GD1a and GD1b, which are the sialic acid positional isomers, these isomers are able to distinguish each other by mean of AP-MALDI-TOF MS spectrometry (Fig. 5a, f) without measurement of MS/MS spectra. In the case of ESI-MS, disialo- and trisialogangliosides have been detected as doubly charged ions, but, in this study, only single charged ions were detected. Vacuum MADLI-MS detected these gangliosides as single charged ions [37], therefore, we conformed this result in AP-MALDI MS analysis.

MALDI-QIT-TOF MS^2 spectra of gangliosides selecting monosialoganglioside ions at *m/z* 1,544 and 1,572 for GM1 (Fig. 2b, d), *m/z* 1,382 and 1,410 for GM2 (Fig. 3b, d), *m/z* 1,382 and 1,410 for GD2 (Fig. 4b, d), *m/z* 1,544 and 1,572 (Fig. 5b, d for GD1a, Fig. 5g, i for GD1b), and *m/z* 1,544 and 1,572 for GT1a (Fig. 6b, d), provide information on carbohydrate sequences of asilao-ganglioside structures quite clearly. When other precursor ions are selected, the ions due to sequential elimination of carbohydrate moieties from deprotonated ions are not obtained so clearly, moreover, the ions responsible for ceramides are not observed clearly, then, it is quite difficult to characterize the structures of the ceramide moieties of gangliosides by following MS^3 analyses.

In the MS^2 mass spectra of GM1, GD1a, GD1b and GT1a gangliosides which are gangliosides having asialo-GM1 backbone structures, two kinds of ions which might be assigned to be $[^{2,3}X_2-2H_2O]^-$ and $[^{0,1}X_2-2H_2O]^-$ due to II-GalNAc ring cleavage of asialo-GM1, are detected. The observation of these ions might be useful for the characterization of asialo-GM1 core structure, because these ions are not observed in the MS^2 spectra of GM2 and GD2 which have asialo-GM2 backbone structure.

In the MS^3 spectra of gangliosides selecting ceramide ions as precursor, significant ions responsible for ceramide fragmentation (P, S, T, U, V, and R shown in Fig. 2) are detected quite clearly with the exception of GD2. In the case of GD2, although only S-ion at *m/z* 324 is not observed in the MS^3 spectrum (Fig. 4c), the ceramide structures can be characterized without any difficulty. The MS^3 spectra by the negative ion AP-MALDI-QIT-TOF system will provide sufficient information on ceramide structure even though in the case of gangliosides which have more complicated molecular species than those of gangliosides used in this study. These results suggest that AP-MALDI-QIT-TOF MS, MS^2 and MS^3 analyses in the negative ion mode provide information on the molecular weight and oligosaccharide sequence, and fatty acid and sphingosine of each ganglioside molecular species. At

present, this method is not suitable for the analysis of ganglioside mixtures, because GD1a, GD1b and GT1b produced GM1 fragment ion, which cannot be distinguished from the ion derived from intact GM1.

Many studies in the research field on the physiological roles of GSLs have been reported. GSLs show heterogeneity not only in their sugar chains but also in their ceramide moieties. The biological significance of ceramide heterogeneity is still not well understood. However, the structure of ceramide could affect the localization and functions of GSLs on the plasma membrane [38, 39]. Therefore, it is important to obtain detailed structural information on ceramides as well as carbohydrate chains of GSLs. Although this method cannot be directly applied to quantitative determination of gangliosides in mixtures, since GM1 fragment ions are produced from disalo- and trisialogangliosides, the method would be a powerful tool for the structural analysis of purified gangliosides, including ceramide structures.

Acknowledgments This work was supported by a grant for Supporting Research Centers in Private Universities and by Grant-in-Aid for Scientific Research (A).

References

1. Hakomori S, Igarashi Y (1995) Functional role of glycosphingolipids in cell recognition and signaling. J Biochem 118:1091–1103
2. Karlsson KA (1998) On the character and functions of sphingolipids. Acta Biochim Pol 45:429–438
3. Maccioni HJ, Quiroga R, Ferrari ML (2011) Cellular and molecular biology of glycosphingolipid glycosylation. J Neurochem 117:589–602
4. Haughey NJ (2010) Sphingolipids in neurodegeneration. Neuromol Med 12:301–305
5. Ledeen R, Wu G (2011) New findings on nuclear gangliosides: overview on metabolism and function. J Neurochem 116: 714–720
6. Dreyfus H, Meuillet E, Guerold B, Fontaine V, Forster V, Heidinger V, Sahel J, Hicks D (1997) Ganglioside and neurotrophic growth factor interactions in retinal neuronal and glial cells. Ind J Biochem Biophys 34:90–96
7. Chiavegatto S, Sun J, Nelson RJ, Schnaar RL (2000) A functional role for complex gangliosides: motor deficits in GM2/GD2 synthase knockout mice. Exp Neurol 166:227–234
8. Rosner H (2003) Developmental expression and possible roles of gangliosides in brain development. Prog Mol Subcell Boil 32:49–73
9. Skaper SD, Leon A, Toffano G (1989) Ganglioside function in the development and repair of the nervous system. From basic science to clinical application. Mol Neurobiol 3:173–199
10. Martin MJ, Martin-Sosa S, Alonso JM, Hueso P (2003) Enterotoxigenic Escherichia coli strains bind bovine milk gangliosides in a ceramide-dependent process. Lipid 38:761–768
11. Ponnusamy S, Meyers-Needham M, Senkal CE, Saddoughi SA, Sentelle D, Selvam SP, Salas A, Ogretmen B (2010) Sphingolipids and cancer: ceramide and sphingosine-1-phosphate in the regulation of cell death and drug resistance. Future Oncol 6: 1603–1624
12. Gault CR, Obeid LM, Hannun YA (2010) An overview of sphingolipid metabolism: from synthesis to breakdown. Adv Exp Med Biol 688:1–23
13. Yang J, Yu Y, Sun S, Duerksen-Hughes PJ (2004) Ceramide and other sphingolipids in cellular responses. Cell Biochem Biophys 40:323–350
14. Ruvolo PP (2003) Intracellular signal transduction pathways activated by ceramide and its metabolites. Pharmacol Res 47: 383–392
15. Levery SB (2005) Glycosphingolipid structural analysis and glycosphingolipidomics. Methods Enzymol 405:300–369
16. Tanaka K, Ojima N, Yamada M (2004) A new approach to post-translational modification analyses using MALDI-QIT-TOF MS. Tanpakushitsu Kakusan Koso 49:1907–1910
17. Yamada K, Kinoshita M, Hayakawa T, Nakaya S, Kakehi K (2009) Comparative studies on the structural features of O-glycans between leukemia and epithelial cell lines. J Proteome Res 8:521–537
18. Laiko VV, Moyer SC, Cotter RJ (2000) Atmospheric pressure MALDI/ion trap mass spectrometry. Anal Chem 72:5239–5243
19. Moyer SC, Cotter RJ, Woods AS (2002) Fragmentation of phosphopeptides by atmospheric pressure MALDI and ESI/Ion trap mass spectrometry. J Am Soc Mass Spectrom 13:274–283
20. Tan PV, Laiko VV, Doroshenko VM (2004) Atmospheric pressure MALDI with pulsed dynamic focusing for high-efficiency transmission of ions into a mass spectrometer. Anal Chem 76:2462–2469
21. Schulz E, Karas M, Rosu F, Gabelica V (2006) Influence of the matrix on analyte fragmentation in atmospheric pressure MALDI. J Am Soc Mass Spectrom 17:1005–1013
22. Navare A, Nouzova M, Noriega FG, Hernández-Martínez S, Menzel C, Fernández FM (2009) On-chip solid-phase extraction pre-concentration/focusing substrates coupled to atmospheric pressure matrix-assisted laser desorption/ionization ion trap mass spectrometry for high sensitivity biomolecule analysis. Rapid Commun Mass Spectrom 23:477–486
23. Suzuki M, Yamakawa T, Suzuki A (1990) High-performance liquid chromatography-mass spectrometry of glycosphingolipids: II. Application to neutral glycolipids and monosialogangliosides. J Biochem 108:92–98
24. Ann Q, Adams J (1992) Structure determination of ceramides and neutral glycosphingolipids by collisional activation of $[M+Lil]^+$ ions. J Am Soc Mass Spectrom 3:260–263
25. Ann Q, Adams J (1993) structure-specific collision-induced fragmentations of ceramides cationized with alkali-metal ions. Anal Chem 65:7–13
26. Lee MH, Lee GH, Yoo JS (2003) Analysis of ceramides in cosmetics by reversed-phase liquid chromatography/electrospray ionization mass spectrometry with collision-induced dissociation. Rapid Commun Mass Spectrom 17:64–75
27. Zarei M, Bindila L, Souady J, Dreisewerd K, Berkenkamp S, Müthing J, Peter-Katalinić J (2008) A sialylation study of mouse brain gangliosides by MALDI a-TOF and o-TOF mass spectrometry. J Mass Spectrom 43:716–725
28. Sugiura Y, Shimma S, Konishi Y, Yamada MK, Setou M (2008) Imaging mass spectrometry technology and application on ganglioside study; visualization of age-dependent accumulation of C20-ganglioside molecular species in the mouse hippocampus. PLoS ONE 3:e3232
29. Laiko VV, Baldwin MA, Burlingame AL (2000) Atmospheric pressure MALDI/ion trap mass spectrometry. Anal Chem 72: 652–657
30. Ikeda K, Taguchi R (2010) Highly sensitive localization analysis of gangliosides and sulfatides including structural isomers in mouse cerebellum sections by combination of laser microdissection and hydrophilic interaction liquid chromatography/

electrospray ionization mass spectrometry with theoretically expanded multiple reaction monitoring. Rapid Commun Mass Spectrom 24:2957–2965
31. Ikeda K, Shimizu T, Taguchi R (2008) Targeted analysis of ganglioside and sulfatide molecular species by LC/ESI-MS/MS with theoretically expanded multiple reaction monitoring. J Lipid Res 49:2678–2689
32. Nakamura K, Suzuki Y, Goto-Inoue N, Yoshida-Noro C, Suzuki A (2006) Structural characterization of neutral glycosphingolipids by thin-layer chromatography coupled to matrix-assisted laser desorption/ionization quadrupole ion trap time-of-flight MS/MS. Anal Chem 78:5736–5748
33. Sugiyama E, Hara A, Uemura K, Taketomi T (1997) Application of matrix-assisted laser desorption ionization time-of-flight mass spectrometry with delayed ion extraction to ganglioside analyses. Glycobiology 7:719–724
34. Mechref Y, Novotny MV (1998) Matrix-assisted laser desorption/ionization mass spectrometry of acidic glycoconjugates facilitated by the use of spermine as a co-matrix. J Am Soc Mass Spectrom 9:1293–1302
35. Jackson SN, Wang HY, Woods AS (2005) Direct profiling of lipid distribution in brain tissue using MALDI-TOFMS. Anal Chem 77:4523–4527
36. Tajiri M, Takeuchi T, Wada Y (2009) Distinct features of matrix-assisted 6 micron infrared laser desorption/ionization mass spectrometry in biomolecular analysis. Anal Chem 81:6750–6755
37. Ivleva VB, Sapp LM, O'Connor PB, Costello CE (2005) Ganglioside analysis by thin-layer chromatography matrix-assisted laser desorption/ionization orthogonal time-of-flight mass spectrometry. J Am Soc Mass Spectrom 16:1552–1560
38. Mahfoud R, Manis A, Binnington B, Ackerley C, Lingwood CA (2010) A major fraction of glycosphingolipids in model and cellular cholesterol-containing membranes is undetectable by their binding proteins. J Biol Chem 285:36049–36059
39. Togayachi A, Kozono Y, Ikehara Y, Ito H, Suzuki N, Tsunoda Y, Abe S, Sato T, Nakamura K, Suzuki M, Goda HM, Ito M, Kudo T, Takahashi S, Narimatsu H (2010) Lack of lacto/neolacto-glycolipids enhances the formation of glycolipid-enriched microdomains, facilitating B cell activation. Proc Natl Acad Sci USA 107:11900–11905